

Photoaffinity Labeling of Mature and Precursor Forms of the Small Subunit of Ribulose-1,5-Bisphosphate Carboxylase/Oxygenase after Expression in *Escherichia coli*¹

Robert R. Klein* and Michael E. Salvucci

United States Department of Agriculture, Agricultural Research Service and Agronomy Department,
University of Kentucky, Lexington, Kentucky 40546–0076

ABSTRACT

The small subunit (SSU) of ribulose-1,5-bisphosphate carboxylase/oxygenase (Rubisco) possesses a binding site that can be photoaffinity labeled with [³²P]8-azidoadenosine 5' triphosphate (N₃ATP). In the present study, photoaffinity labeling was used to compare the nucleotide analog binding properties of SSU in the Rubisco holoenzyme complex (holoE SSU) with the properties of isolated SSU and the precursor form (pSSU) that contains a transit peptide. To facilitate these studies, the complete coding regions of tobacco (*Nicotiana tabacum* L.) SSU and pSSU were cloned into pET expression vectors and the polypeptides were synthesized in *Escherichia coli*. Protein import studies showed that cloned pSSU polypeptides were imported into intact chloroplasts, where they were processed to the mature form and assembled into the Rubisco holoenzyme. Cloned SSU and pSSU isolated from *E. coli* were photoaffinity labeled with N₃ATP. The apparent K_D value for SSU and pSSU, 18 micromolar N₃ATP, was identical to the value determined for holoE SSU. However, differences in photolabeling between cloned SSU or pSSU and holoE SSU were apparent in the level of protection afforded by ATP and UTP, in the response of photolabeling to free Mg²⁺, and in the higher photolabeling efficiency that characterized the cloned SSU. Treatment of the Rubisco holoenzyme with a concentration of urea sufficient to disassociate the subunits markedly increased photoincorporation into SSU, indicating that intersubunit associations within the holoenzyme complex may be the major factor influencing photolabeling efficiency of SSU. Thus, differences in SSU conformation between the isolated and assembled states affect photolabeling efficiency and other nucleotide analog binding properties of the SSU, but not the apparent affinity for N₃ATP.

The higher plant type Rubisco (EC 4.1.1.39) comprises eight 53 kD LSU² and eight 14 kD SSU (reviewed in ref. 3). The active site of the enzyme is situated on the LSU, formed by amino- and carboxy-terminal domains of adjacent subunits (1, 6, 11, 13). Small subunits are grouped as pairs of

dimers on two ends of the LSU core complex (6, 13), but despite extensive interactions with LSU, they do not contribute residues to the active site (1, 13). Andrews *et al.* (4) have shown that SSU participate directly or indirectly in the three partial reactions of catalysis, although a precise role in the reaction mechanism has not been elucidated. From the high resolution crystal structure of the enzyme, it appears that SSU interacts with regions of the LSU that determine the active site geometry, particularly a helical loop region that is in close proximity to one of the phosphates of the substrate (20). Based upon this observation, it has been proposed that SSU affects catalysis by interacting with regions of the LSU that influence substrate binding (20). Reconstitution experiments with the cyanobacterial enzyme have lent support to this idea by demonstrating an influence of SSU on maintaining the stability of the tight binding of the reaction intermediate analog 2-carboxyarabinitol 1,5-bisphosphate to the active site (21).

An interesting feature of the Rubisco SSU is that it can be photoaffinity labeled by the nucleotide analog 8-N₃ATP (18). Saturation kinetic behavior, a K_D for photoincorporation in the micromolar range, and the extremely low incorporation with 8-N₃GTP compared with 8-N₃ATP all indicate the presence of a specific binding site on the SSU. In photoaffinity labeling studies, competition binding is used to reveal the identity of the native substrate for the site (16). However, ATP, ADP, UTP, and other common nucleotides afforded little protection against photolabeling (18). Thus, the physiological significance of the site and its relationship to the role of the SSU in catalysis is unknown pending identification of the native substrate.

Several possible functions can be proposed for the photoaffinity site on the SSU based upon the reported interactions of Rubisco with nucleotides. These functions include SSU transport (7), holoenzyme assembly (5), and Rubisco activation (23). Alternatively, the binding site on the SSU may not be a nucleotide binding site at all but instead may be specific for some other type of molecule (18). To evaluate the physiological role of the SSU binding site, we used photoaffinity labeling to compare the nucleotide analog binding properties of isolated SSU, pSSU, which contains a transit peptide, and holoE SSU. The results presented herein provide the basis for mutational analysis of the SSU binding site for elucidation of its function.

¹ Kentucky Agricultural Experiment Station Journal Series No. 91–3–126. This work was supported by a cooperative grant from the U.S. Department of Agriculture.

² Abbreviations: LSU, large subunit(s) of Rubisco; SSU, small subunit(s) of Rubisco; N₃ATP, azidoadenosine 5'-triphosphate; pSSU, small subunit precursor(s); holoE SSU, small subunit assembled in the holoenzyme complex; PCR, polymerase chain reaction; IPTG, isopropyl-β-thiogalactoside; IgG, immunoglobulin G.

MATERIALS AND METHODS

Biochemicals

[γ - ^{32}P]8-N₃ATP was synthesized as described by Potter and Haley (16) and was a generous gift from Dr. Boyd E. Haley (University of Kentucky). [^{35}S]Methionine was purchased from New England Nuclear (DuPont Co., Wilmington, DE).³ Except where indicated below, all other reagents were from Sigma Chemical Co.

Isolation of Rubisco

Rubisco was isolated from tobacco (*Nicotiana tabacum* L. cv KY 14) leaves by the procedure described previously (9) with the following modification: gel filtration chromatography was replaced by zonal sedimentation in sucrose gradients (8). Rubisco isolated by this procedure was stored as a frozen (NH₄)₂SO₄ suspension. For photoaffinity labeling experiments, precipitated protein was collected from the thawed suspension by centrifugation and was resuspended at 4°C in 50 mM Tris-HCl, 5 mM MgCl₂, pH 7.6 (buffer A) containing 10 mM 2-mercaptoethanol. The solution was dialyzed overnight at 4°C against 20 mM Tris-HCl, 5 mM MgCl₂, pH 7.6 (buffer B) before storage in aliquots at -80°C.

Screening of Lambda ZAP II cDNA Library and Analysis of Amplified DNA Products

A Lambda ZAP II tobacco cDNA library (Stratagene, La Jolla, CA) was screened for *rbcS* sequences by PCR amplification (10). The PCR amplification strategy for cloning *rbcS* is outlined in Figure 1. One-microliter aliquots of a tobacco cDNA library (1.8×10^6 recombinants) were placed in reaction tubes and brought to 74 μL with water. Phage particles were disrupted by heating to 100°C for 5 min and then were placed on ice. Twenty-six microliters of a master mix was added to each reaction tube to give the PCR conditions of 10 mM Tris-HCl (pH 8.3), 50 mM KCl, 1.5 mM MgCl₂, 0.001% gelatin, 0.2 mM each dNTP, 100 pmol each oligonucleotide primer, and 2.5 units Taq DNA polymerase (Perkin Elmer Cetus, Norwalk, CT). Thermal cycling was conducted for 30 cycles as follows: 94°C, 1 min 20 sec (denaturation); 57°C, 2 min (annealing); 72°C for 3 min (primer extension). Oligonucleotide primers for amplifying the coding regions of pSSU and SSU were selected using the OLIGO DNA Amplification Program (17). To permit cloning of pSSU and SSU coding region in pET expression plasmids (Novagen, Madison, WI), *Nde*I or *Nco*I restriction sites were created at the 5' end of the sense primer and a *Eco*RV restriction site created at the 5' end of the antisense primer. Following thermal cycling, amplified DNA sequences were analyzed on agarose gels and PCR products were gel purified by the GENECLEAN protocol (BIO-101, La Jolla, CA). SSU and pSSU sequences were

blunt-end cloned into SK plasmids (Stratagene). Single strand phagemid templates were prepared using the helper phage M13K07. The nucleotide sequences of SSU and pSSU clones were determined by the dideoxynucleotide chain termination method (19) using Sequenase (U.S. Biochemical Corp, Cleveland, OH). After sequencing, pSSU and SSU sequences were subcloned into pET 11 plasmids. SSU and pSSU proteins were synthesized in *Escherichia coli* as described (24).

Isolation and Solubilization of the SSU and pSSU

After induction with IPTG (24), *E. coli* cells were harvested by centrifugation at 10,000g for 5 min, resuspended at 4°C in buffer A, and frozen at -80°C. The cells were thawed on ice and disrupted at 4°C by sonication. Inclusion bodies were collected by centrifugation at 10,000g for 10 min and resuspended at 4°C in buffer A containing 1% Triton X-100. After collection by centrifugation, inclusion bodies were solubilized at room temperature by resuspension in buffer A containing 8 M urea and 10 mM 2-mercaptoethanol. After 5 min, insoluble material was removed by centrifugation for 10 min at 13,000g. The supernatant was dialyzed at 4°C against buffer B. After 18 h, the dialysate was centrifuged for 10 min at 13,000g and the supernatant, which contained nearly all of the SSU and pSSU, was divided into aliquots before storage at -80°C. Preliminary experiments showed that no changes in photoaffinity labeling occurred when SSU and pSSU were frozen and stored for at least 3 months at -80°C.

In Vitro pSSU Uptake into Tobacco Chloroplasts

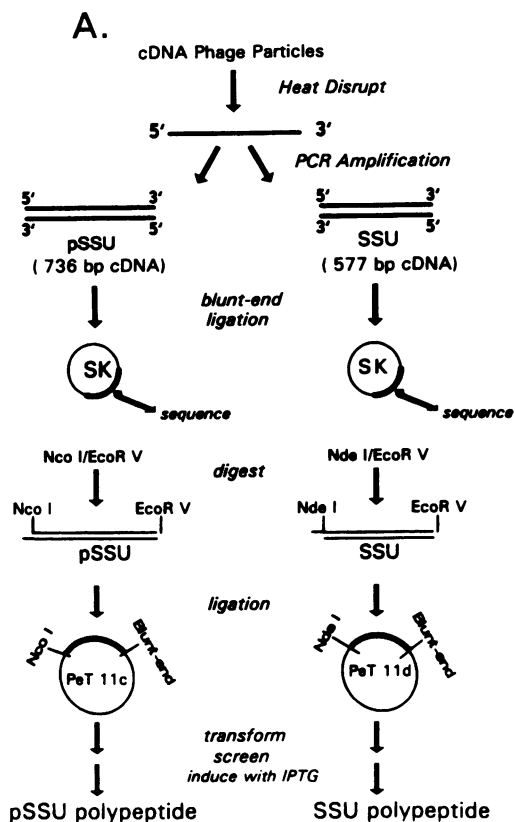
SSU and pSSU polypeptides were radiolabeled with [^{35}S]methionine in *E. coli*. Cells containing recombinant pET plasmids were induced with IPTG at an $A_{600\text{nm}} = 0.7$. After 15 min, 150 μCi of [^{35}S]methionine (1151.4 Ci/mmol) was added to each 5 mL culture and incubated at 37°C for 1.5 to 2 h. ^{35}S -labeled pSSU and SSU polypeptides were purified from these cultures as detailed above.

Intact chloroplasts were isolated from 3-week-old tobacco (*Nicotiana rustica* L., cv Pumila) seedlings as described (12) and incubated with ^{35}S -labeled SSU or pSSU. The conditions for *in vitro* protein uptake by isolated intact chloroplasts were as described by Cline *et al.* (7). After 30 min, plastids were treated with thermolysin and intact chloroplasts were reisolated. Chloroplasts were fractionated into membrane and stromal phases (12) and the fractions were electrophoresed on 7.5 to 15% SDS-PAGE gels (14) or on 5 to 18% native PAGE gels without the addition of SDS or 2-mercaptoethanol (14). Gels were subsequently stained, impregnated with fluor, and exposed to x-ray film (12).

Photoaffinity Labeling

Unless indicated otherwise in the text, photoaffinity labeling of SSU, pSSU, and the Rubisco holoenzyme was performed in microfuge tubes at 4°C in 25 μL buffer B containing 10 mM EDTA, 10 μM [^{32}P]N₃ATP, and a protein concentra-

³ Mention of a trademark, proprietary product, or vendor does not constitute a guarantee or warranty of the product by the U.S. Department of Agriculture and does not imply its approval to the exclusion of other products or vendors that may also be suitable.

**B.****SSU Sense Primer:**

Met Gln Val Trp Pro Pro Ile Asn
5' GAG CAT ATG CAG GTG TGG CCA CCA ATT AAC 3'
Nde I

pSSU Sense Primer:

Met Ala Ser Ser Val Leu Ser Ser
5' GAG ACC ATG GCT TCC TCA GTT CTT TCC TCT 3'
Nco I

Antisense Primer:

5' CCG GAT ATC AAA CAA AGC ACC AAA TCA TAA T 3'
EcoR V

Figure 1. Strategy for PCR screening and cloning of *rbcS* cDNA sequences. A, Schematic steps in PCR amplification and cloning *rbcS* cDNAs. B, Selection of PCR primers for amplification of pSSU and SSU sequences. The sense primers were synthesized to the eight N-terminal amino acids. To permit cloning into pET II expression vectors, *Nco*I (pSSU) or *Nde*I (SSU) linkers were designed at the 5' end of sense primers. The antisense primers were synthesized to a sequence in the 3' untranslated region of *rbcS*. To permit blunt-end ligation (3' end of gene) of pSSU and SSU sequences into pET II vector, a *EcoRV* linker was designed at the 5' end of the antisense primer.

tion of 30 to 100 pmol. Reactions were initiated by addition of the labeled photoprobe. After 15 s, the reactions were irradiated for 1 min with 3000 μ W of 254 nm radiation and terminated by the addition of SDS and DTT (18). Labeled polypeptides were separated by SDS-PAGE on 13% minigels or 7.5 to 15% linear gradient gels (18) and visualized by staining with Coomassie brilliant blue R-120. Gels were dried between plastic film (BioGelwrap, Biodesign Inc., Carmel, NY) and exposed to x-ray film. Autoradiographic exposures in the linear range of the emulsion were scanned with a BioImage image acquisition densitometer (MilliGen/Bio-search, Ann Arbor, MI), which quantified the amount of 32 P incorporation into each polypeptide by integrating intensity in the entire band.

Quantitation of Rubisco Holoenzyme, pSSU, and SSU Protein, and Photoincorporation

Tobacco Rubisco holoenzyme protein was determined from the absorbance at 280 nm (18). The amounts of pSSU and SSU were determined densitometrically from the integrated intensity of the corresponding bands on Coomassie blue-stained SDS-PAGE gels. Rubisco holoenzyme was used to construct a standard curve for SSU protein and the

amounts of SSU and pSSU were determined over the linear portion of the curve. The relative amounts of SSU and pSSU determined by Coomassie blue staining were similar to the amounts determined by densitometric scanning of western blots (9). 32 P incorporation into cloned SSU and pSSU and holoE SSU was determined after separation of the polypeptides by SDS-PAGE. The stained bands were excised from the gel and 32 P dpm were determined by liquid scintillation spectroscopy.

Miscellaneous

Electrophoretic transfer of proteins after SDS-PAGE and western blot analysis was conducted as described previously (9). Blots were visualized using anti-tobacco (holoenzyme) IgG (9). Horizontal isoelectric focusing was performed at 10°C in precast 0.6 mm agarose gels over a pH range of 3 to 7 according to the manufacturer's instructions (FMC Bio-Products, Rockland, ME).

RESULTS

PCR Amplification and Analyses of *rbcS* Sequences

PCR technology was used to screen a tobacco cDNA library for pSSU and SSU coding sequences (Fig. 1). The tobacco

genomic *rbcS* sequence reported by Mazur and Chui (15) was used to select homologous oligonucleotide primers for PCR amplification. The forward (sense) primers (5' end of gene) were positioned at the nucleotide sequences encoding the N-terminus of pSSU or SSU proteins. The reverse (antisense) primer was positioned in the 3' untranslated region of the *rbcS* gene. PCR amplification of pSSU and SSU nucleotide sequences yielded single PCR products of 736 and 577 base pairs, respectively (data not shown). DNA sequence analysis confirmed the PCR products as coding for pSSU or SSU polypeptides. Comparison of the present sequences with the tobacco genomic *rbcS* sequence of Mazur and Chui (15) revealed six single-nucleotide differences. All differences were either silent third position changes or occurred in the 3' untranslated region.

Overexpression of SSU and pSSU in *E. coli*

Cloning of pSSU and SSU coding sequences into the pET T7 expression system permitted pSSU and SSU polypeptide production in *E. coli*. When *E. coli* cells were incubated for 2 h with IPTG, target polypeptides of 24 and 14 kD accumulated in cells harboring the recombinant pSSU and SSU pET T7 plasmids, respectively (Fig. 2A). These polypeptides represented greater than 20% of the total cellular protein in *E. coli* on the basis of their Coomassie blue staining intensity. Western blot analysis with anti-Rubisco IgG confirmed the identity of the 14 and 24 kD polypeptides as SSU and pSSU, respectively (Fig. 2B). Isoelectric focusing in 8 M urea showed that the isoelectric point of the cloned SSU was identical to

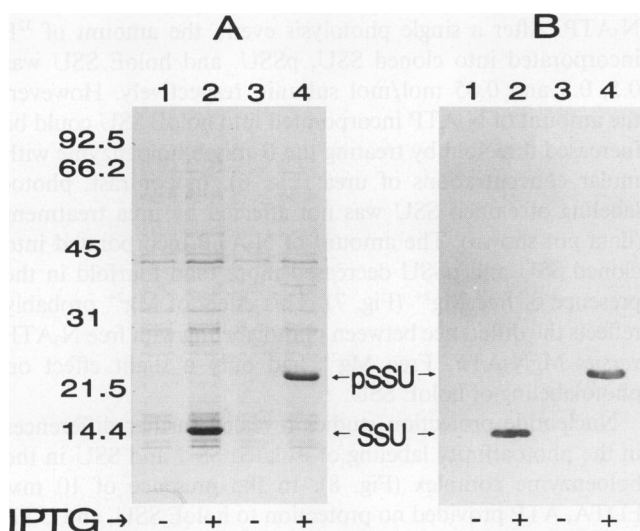


Figure 2. Synthesis of pSSU and SSU polypeptides in *E. coli*. A, Coomassie blue-stained SDS-PAGE gel of *E. coli* polypeptides. Polypeptides in lanes 1 and 2 were synthesized in cells containing recombinant SSU pET plasmids, and lanes 3 and 4 contained pSSU pET plasmids, either before (lanes 1 and 3) or after (lanes 2 and 4) the addition of IPTG. B, Western blot analysis of *E. coli* polypeptides. Polypeptides shown in A were reacted with anti-Rubisco (holoenzyme) IgG after electrophoretic transfer to nitrocellulose. Lane designation same as in A.

the isoelectric point of one of two SSU isoforms present in the Rubisco holoenzyme (data not shown).

Following induction of pSSU or SSU synthesis in *E. coli*, virtually all of the SSU and pSSU was localized in inclusion bodies. Protein in the inclusion bodies could be solubilized by treatment with either 8 M urea or 6 M guanidine-HCl. The SSU and pSSU remained completely soluble when dialyzed overnight against a 1000-fold excess of buffer, although other proteins associated with the inclusion bodies precipitated upon dialysis. After centrifugation, the SSU and pSSU comprised greater than 90% of the solubilized protein from the inclusion bodies (see Figs. 3 and 4).

Chloroplast Import and Assembly

To assess the effect of urea solubilization on the Rubisco SSU polypeptides, the ability of urea-solubilized pSSU to be imported into isolated tobacco chloroplasts was determined (Fig. 3). When ^{35}S -labeled pSSU were incubated with intact tobacco chloroplasts, pSSU polypeptides were transported into plastids and were processed to the mature, 14 kD form (Fig. 3A, lanes 2 and 3 versus 4). Most of the imported SSU were localized in the stromal phase. As a control, mature SSU polypeptides were also used for uptake experiments. Import of ^{35}S -labeled SSU into tobacco chloroplasts (Fig. 3A) and assembly into the holoenzyme (Fig. 3B) were not detected.

To determine if imported SSU were assembled into the Rubisco holoenzyme, the stromal phase was electrophoresed on a nondenaturing gel after import of ^{35}S -labeled pSSU (Fig. 3B). Autoradiography showed that most of the label from imported SSU was associated with a single high mol wt protein (Fig. 3B, lane 4). This protein comigrated with the Rubisco holoenzyme as determined by Coomassie blue stain (Fig. 3B, lanes 1 and 2). A small portion of the label was associated with a smaller unidentified band (marked with asterisk), presumably unassembled SSU.

Photoaffinity Labeling Studies

Photoaffinity labeling with $[^{32}\text{P}]\text{N}_3\text{ATP}$ was conducted with cloned SSU and pSSU proteins isolated from *E. coli* and with Rubisco holoenzyme isolated from tobacco leaves (Fig. 4). Cloned SSU and pSSU were labeled when irradiated in the presence of 10 μM N_3ATP (Fig. 4B, lanes 4 and 6) as were both subunits of the Rubisco holoenzyme (Fig. 4B, lane 2). In all cases, ^{32}P incorporation was dependent upon irradiation with UV light because no incorporation was observed when proteins were incubated with N_3ATP but not photolyzed (Fig. 4B, lanes 1, 3, and 5). The addition of 8 mM urea, the approximate amount remaining in the SSU and pSSU preparations after dialysis, had no effect on photoincorporation of N_3ATP into either subunit of tobacco Rubisco (data not shown).

The effect of N_3ATP concentration on photoaffinity labeling of cloned SSU and pSSU and holoE SSU was examined (Fig. 5). The response of photoincorporation to N_3ATP concentration was virtually identical for the three proteins. Photoincorporation in response to N_3ATP concentration exhibited saturation kinetic behavior with an apparent K_D value of 18 μM .

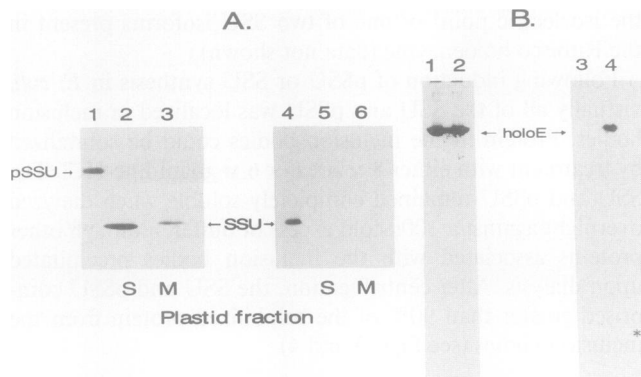


Figure 3. *In vitro* pSSU uptake into isolated chloroplasts and assembly into Rubisco holoenzyme. A, Autoradiogram of protein import. [³⁵S]Methionine-labeled pSSU (lane 1) or SSU (lane 4) were incubated with intact tobacco chloroplasts for 30 min. Chloroplasts incubated with radiolabeled pSSU were fractionated into stromal (S, lane 2) and membrane (M, lane 3) fractions. Chloroplasts incubated with radiolabeled SSU were also fractionated into stromal (lane 5) or membrane (lane 6) fractions. Samples were electrophoresed, impregnated with fluor, and exposed to x-ray film. B, Nondenaturing gel of stromal fractions after protein uptake. Following *in vitro* uptake and plastid fractionation, stromal samples were electrophoresed on 5 to 18% PAGE gel and either stained with Coomassie blue (lanes 1 and 2) or impregnated with fluor and exposed to x-ray film (lanes 3 and 4). Lanes 1 and 3 represent stromal fraction of plastids incubated with radiolabeled SSU and lanes 2 and 4 the stromal fractions of plastids incubated with radiolabeled pSSU.

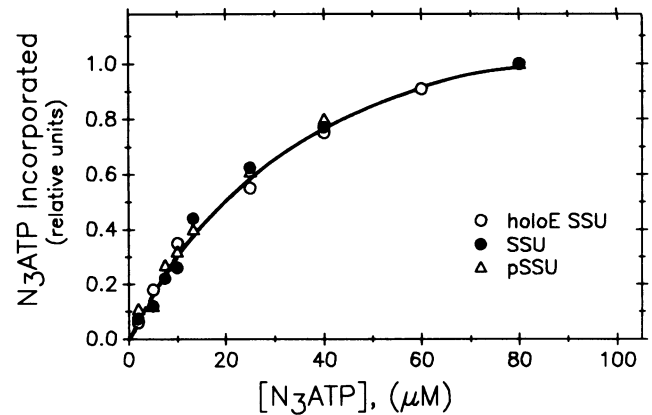


Figure 5. Concentration dependence of photoaffinity labeling of cloned SSU, pSSU, and holoE SSU. Cloned SSU (●), pSSU (Δ), and purified tobacco Rubisco (○) were photolyzed in the presence of the indicated concentrations of N₃ATP and the polypeptides were separated by SDS-PAGE. Incorporation was determined from densitometer scans of the autoradiograms and was normalized to the level measured at 80 μM.

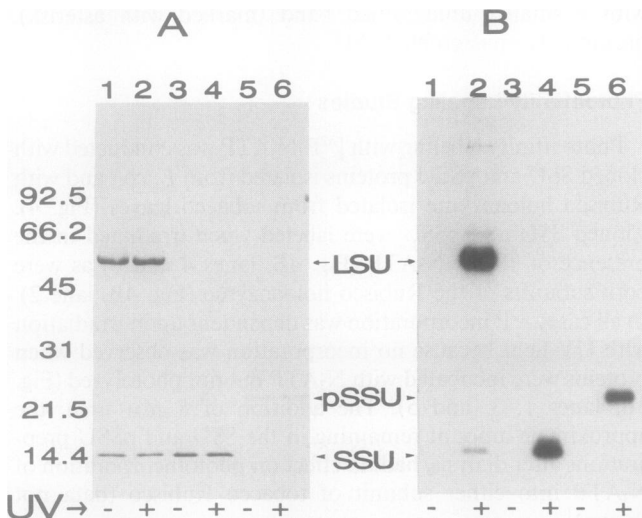


Figure 4. Photoaffinity labeling of cloned SSU and pSSU and purified tobacco leaf Rubisco. Polypeptides were separated by SDS-PAGE after incubation of purified Rubisco isolated from tobacco leaves (lanes 1 and 2), SSU (lanes 3 and 4), and pSSU (lanes 5 and 6) with 10 μM [³²P]N₃ATP. Reactions were either kept dark (lanes 1, 3, and 5) or photolyzed (lanes 2, 4, and 6). A, Coomassie blue-stained gel. B, Autoradiogram.

Although cloned SSU and pSSU and holoE SSU exhibited the same apparent affinity for N₃ATP, the amount of N₃ATP incorporated into SSU or pSSU polypeptides appeared to be considerably higher than the amount incorporated into the holoE SSU based upon their relative staining intensities (compare Fig. 4A and B). This conclusion was confirmed when photolabeling efficiency (mol ³²P incorporated/mol protein) was measured directly using a saturating concentration of N₃ATP. After a single photolysis event, the amount of ³²P incorporated into cloned SSU, pSSU, and holoE SSU was 0.5, 0.3 and 0.05 mol/mol subunit, respectively. However, the amount of N₃ATP incorporated into holoE SSU could be increased threefold by treating the Rubisco holoenzyme with molar concentrations of urea (Fig. 6). In contrast, photolabeling of cloned SSU was not affected by urea treatment (data not shown). The amount of N₃ATP incorporated into cloned SSU and pSSU decreased more than fourfold in the presence of free Mg²⁺ (Fig. 7). This effect of Mg²⁺ probably reflects the difference between photolabeling with free N₃ATP versus MgN₃ATP. Free Mg²⁺ had only a slight effect on photolabeling of holoE SSU.

Nucleotide protection studies revealed further differences in the photoaffinity labeling of isolated SSU and SSU in the holoenzyme complex (Fig. 8). In the presence of 10 mM EDTA, ATP provided no protection to holoE SSU, and UTP blocked photoincorporation by only 30%. In contrast, ATP and UTP blocked photoincorporation of N₃ATP into cloned SSU and pSSU by 50 and 40%, respectively. In the presence of free Mg²⁺, ATP and UTP afforded a relatively high level of protection to holoE SSU, 80 and 70%, respectively. However, to achieve this level of protection, ATP and UTP had to be present at concentrations that were high (500 μM) relative to the K_D for photolabeling (18 μM). Compared with the effect on holoE SSU, ATP and UTP were less effective in blocking

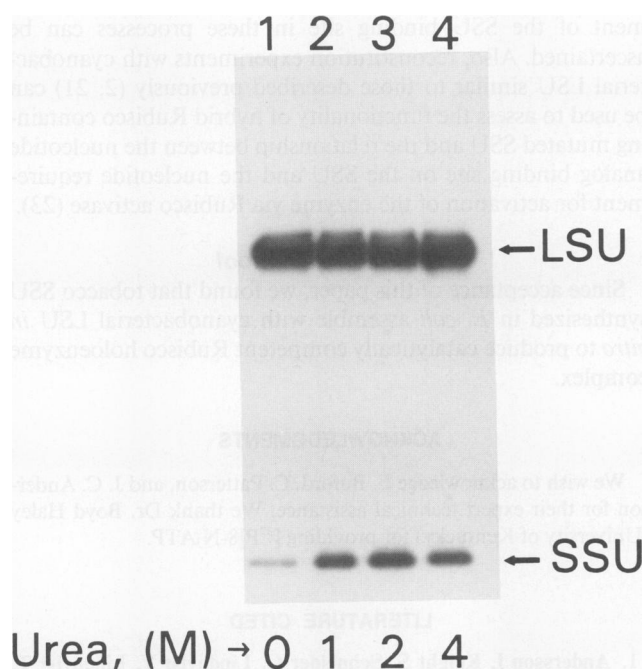


Figure 6. Effect of urea on photoincorporation of [^{32}P]N $_3$ ATP into the subunits of purified tobacco Rubisco. Autoradiogram of labeled LSU and SSU polypeptides separated by SDS-PAGE after photolabeling purified Rubisco with 10 μM [^{32}P]N $_3$ ATP in the presence of the indicated concentrations of urea.

photoincorporation into cloned SSU or pSSU in the presence of free Mg^{2+} .

DISCUSSION

Photoaffinity labeling with 8-N $_3$ ATP has been used to identify nucleotide-binding proteins in a number of biological systems and to characterize the nucleotide-binding properties of the subunits of attachment (16). Previously (18), photoaffinity labeling with N $_3$ ATP covalently modified Rubisco at the active site and revealed a putative binding site on the SSU. The physiological function of the binding site on the SSU has not been determined. To facilitate an analysis of the nucleotide analog binding properties of the SSU, the coding region of the SSU was cloned into a pET T7 expression vector. The pET T7 expression vector permits expression of a full-length target protein in *E. coli* without attachment of a fusion peptide (24). For comparative analysis, the pSSU was also produced in *E. coli*. The synthesis of pSSU and SSU polypeptides permitted a direct comparison of the nucleotide binding properties of SSU in its isolated and assembled forms.

The T7 promoter directed *E. coli* to synthesize relatively high levels of SSU and pSSU. A consequence of the high level of expression was the packaging of pSSU and SSU into inclusion bodies that required treatment with urea for solubilization. After removal of the urea by dialysis, the pSSU polypeptides renatured to the correct conformation for transport across the chloroplast envelope and for assembly into the holoenzyme complex. In a previous study, Smrcka *et al.* (22)

showed that even after urea solubilization, cloned SSU from the cyanobacterium *Synechococcus* and from pea assembled spontaneously with the *Synechococcus* LSU core complex to produce catalytically active Rubisco. These observations together with our results indicate that SSU and pSSU treated with urea fold properly to a functional conformation once the denaturant is removed.

Photoaffinity labeling of isolated SSU and pSSU with the nucleotide analog N $_3$ ATP confirmed the previous conclusion that the binding site on the SSU is not formed by interaction with LSU (18). The K_D values for photoincorporation into SSU and pSSU were identical and similar to the value for holoE SSU. Thus, assembly into a holoenzyme complex or addition of the transit peptide did not affect the overall affinity of the binding site on the SSU for N $_3$ ATP.

Although the affinity of the SSU binding site for N $_3$ ATP was virtually identical for the isolated and assembled states, cloned SSU and holoE SSU exhibited major differences in photolabeling efficiency and in the response of photolabeling to Mg^{2+} and nucleotides. The difference in photolabeling efficiency appeared to be due to intersubunit associations in the holoenzyme complex because treatment of the holoenzyme with concentrations of urea sufficient to dissociate the subunits markedly increased the photolabeling efficiency of holoE SSU. In contrast, addition of the transit peptide had much less of an effect on photolabeling efficiency or on the level of protection afforded by ATP and UTP. Because the efficiency of photolabeling depends upon the proximity of residues with which to form a stable covalent bond (16), the

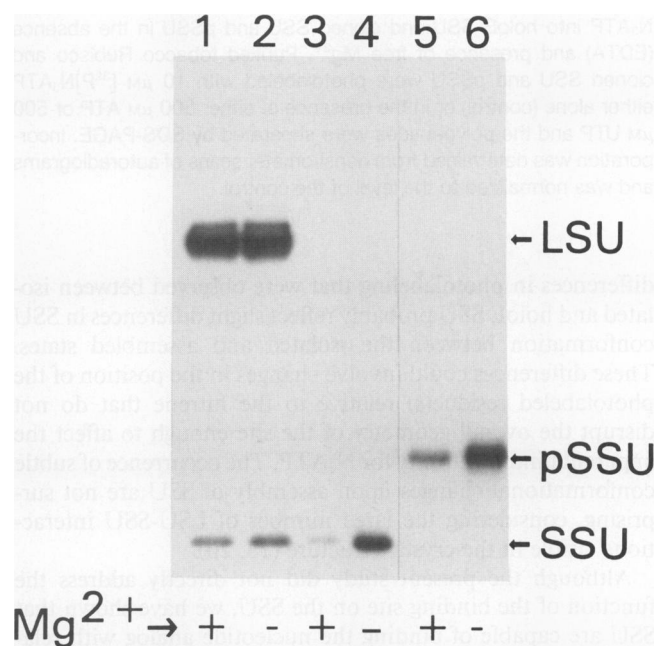


Figure 7. Effect of free Mg^{2+} on photoincorporation of [^{32}P]N $_3$ ATP into the subunits of purified tobacco Rubisco and cloned SSU and pSSU. Autoradiogram of labeled polypeptides separated by SDS-PAGE after photolabeling purified Rubisco (lanes 1 and 2), cloned SSU (lanes 3 and 4), and pSSU (lanes 5 and 6) with 10 μM [^{32}P]N $_3$ ATP in the presence of 5 mM Mg^{2+} (lanes 1, 3, and 5) or 4 mM Mg^{2+} plus 10 mM EDTA (lanes 2, 4, and 6).

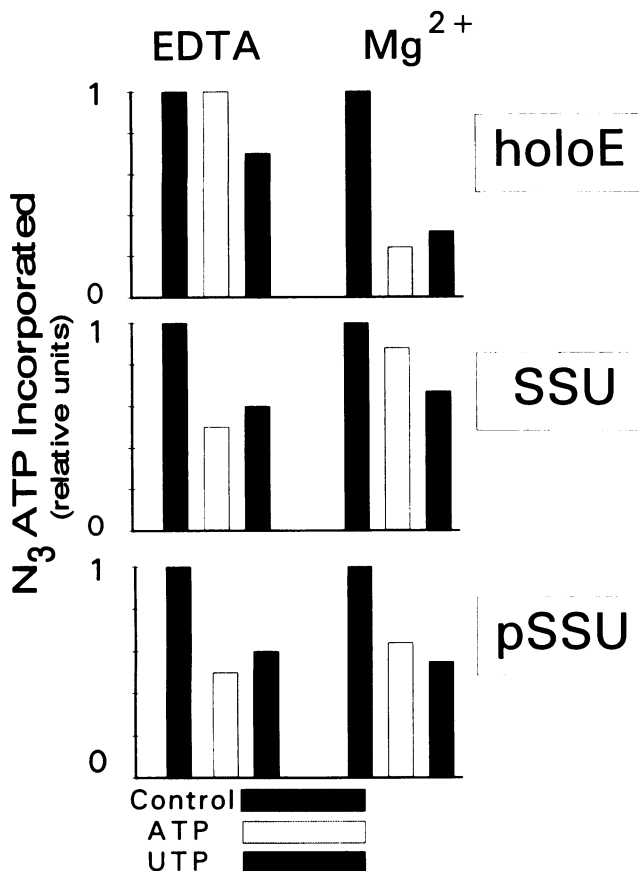


Figure 8. Effect of ATP and UTP on photoincorporation of [³²P] N₃ATP into holoE SSU and cloned SSU and pSSU in the absence (EDTA) and presence of free Mg²⁺. Purified tobacco Rubisco and cloned SSU and pSSU were photolabeled with 10 μM [³²P]N₃ATP either alone (control) or in the presence of either 500 μM ATP or 500 μM UTP and the polypeptides were separated by SDS-PAGE. Incorporation was determined from densitometer scans of autoradiograms and was normalized to the level of the control.

differences in photolabeling that were observed between isolated and holoE SSU probably reflect slight differences in SSU conformation between the isolated and assembled states. These differences could involve changes in the position of the photolabeled residue(s) relative to the nitrene that do not disrupt the overall geometry of the site enough to affect the apparent binding affinity for N₃ATP. The occurrence of subtle conformational changes upon assembly of SSU are not surprising, considering the large number of LSU-SSU interactions visible in the crystal structure (13, 20).

Although the present study did not directly address the function of the binding site on the SSU, we have shown that SSU are capable of binding the nucleotide analog with relatively high affinity in the isolated state and when bearing a transit peptide. With the expression system described here, mutations can be introduced into the SSU sequence to alter nucleotide analog binding. By examining the ability of mutated SSU to be transported across the chloroplast envelopes and assembled into the holoenzyme complex, the involve-

ment of the SSU binding site in these processes can be ascertained. Also, reconstitution experiments with cyanobacterial LSU similar to those described previously (2, 21) can be used to assess the functionality of hybrid Rubisco containing mutated SSU and the relationship between the nucleotide analog binding site on the SSU and the nucleotide requirement for activation of the enzyme via Rubisco activase (23).

Note Added in Proof

Since acceptance of this paper, we found that tobacco SSU synthesized in *E. coli* assemble with cyanobacterial LSU *in vitro* to produce catalytically competent Rubisco holoenzyme complex.

ACKNOWLEDGMENTS

We wish to acknowledge E. Buford, C. Patterson, and J. C. Anderson for their expert technical assistance. We thank Dr. Boyd Haley (University of Kentucky) for providing [³²P]8-N₃ATP.

LITERATURE CITED

- Andersson I, Knight S, Schneider G, Lindqvist Y, Lindqvist T, Branden C-I, Lorimer GH (1989) Crystal structure of the active site of ribulose-bisphosphate carboxylase. *Nature* **337**: 229–234
- Andrews TJ, Lorimer GH (1985) Catalytic properties of a hybrid between cyanobacterial large subunits and higher plant small subunits of ribulose bisphosphate carboxylase-oxygenase. *J Biol Chem* **260**: 4632–4636
- Andrews TJ, Lorimer GH (1987) Rubisco: structure, mechanisms and prospects for improvement. In MD Hatch, NK Boardman, eds, *The Biochemistry of Plants*, Vol 13. Academic Press, New York, pp 131–218
- Andrews TJ, Lorimer GH, Pierce J (1986) Three partial reactions of ribulose-bisphosphate carboxylase require both large and small subunits. *J Biol Chem* **261**: 12184–12188
- Bloom MV, Milos P, Roy H (1983) Light-dependent assembly of ribulose-1,5-bisphosphate carboxylase. *Proc Natl Acad Sci USA* **80**: 1013–1017
- Chapman MS, Suh SW, Cascio D, Smith WW, Eisenberg D (1987) Sliding-layer conformational change limited by quaternary structure of plant RuBisCO. *Nature* **329**: 354–356
- Cline K, Werner-Washburne M, Lubben TH, Keegstra K (1985) Precursors to two nuclear-encoded chloroplast proteins bind to the outer envelope membrane before being imported into chloroplasts. *J Biol Chem* **260**: 3691–3696
- Covey SN, Taylor SC (1980) Rapid purification of ribulose 1,5-bis(phosphate) carboxylase from *Rhodospirillum rubrum*. *FEMS Microb Lett* **8**: 221–223
- Crafts-Brandner SJ, Salvucci ME, Egli DB (1989) Changes in ribulosebisphosphate carboxylase/oxygenase and ribulose 5-phosphate kinase abundances and photosynthetic capacity during leaf senescence. *Photosynth Res* **23**: 223–230
- Friedman KD, Rosen NL, Newman PJ, Montgomery RR (1990) Screening of λgt11 libraries. In MA Innis, Dh Gelfand, JJ Sninsky, TJ White, eds, *PCR Protocols: A Guide to Methods and Applications*. Academic Press, San Diego, pp 253–258
- Lee EH, Soper TS, Mural RJ, Stringer CD, Hartman FC (1987) An intersubunit interaction at the active-site of D-ribulose-1,5-bisphosphate carboxylase/oxygenase as revealed by cross-linking and site-directed mutagenesis. *Biochemistry* **26**: 4599–4604
- Klein RR, Mullet JE (1986) Regulation of chloroplast-encoded chlorophyll-binding protein translation during higher plant chloroplast biogenesis. *J Biol Chem* **261**: 11138–11145

13. Knight S, Andersson I, Branden C-I (1990) Crystallographic analysis of ribulose 1,5-bisphosphate carboxylase from spinach at 2.4 Å resolution. Subunit interactions and active site. *J Mol Biol* **215**: 113–160
14. Laemmli UK (1970) Cleavage of structural proteins during the assembly of the head of bacteriophage T4. *Nature* **227**: 680–685
15. Mazur BJ, Chui C-F (1985) Sequence of a genomic DNA clone for the small subunit of ribulose biphosphate carboxylase-oxygenase from tobacco. *Nucleic Acids Res* **13**: 2373–2386
16. Potter RL, Haley BE (1983) Photoaffinity labeling of nucleotide binding sites with 8-azidopurine analogs: techniques and applications. *Methods Enzymol* **91**: 613–633
17. Rychlik W, Rhoads RE (1989) A computer program for choosing optimal oligonucleotides for filter hybridization, sequencing and *in vitro* amplification of DNA. *Nucleic Acids Res* **17**: 8543–8551
18. Salvucci ME, Haley BE (1990) Photoaffinity labeling of ribulose-bisphosphate carboxylase/oxygenase with 8-azidoadenosine 5'-triphosphate. *Planta* **181**: 287–295
19. Sambrook J, Fritsch EF, Maniatis T (1989) *Molecular Cloning*. Cold Spring Harbor Laboratory, Cold Spring Harbor, NY
20. Schneider G, Knight S, Andersson I, Branden C-I, Lindqvist Y, Lindqvist T (1990) Comparison of the crystal structures of L₂ and L₈S₈ Rubisco suggests a functional role for the small subunit. *EMBO J* **9**: 2045–2050
21. Smrcka AV, Bohnert HJ, Jensen RG (1991) Modulation of the tight binding of carboxyarabinitol 1,5-bisphosphate to the large subunit of ribulose 1,5-bisphosphate carboxylase/oxygenase. *Arch Biochem Biophys* **286**: 14–19
22. Smrcka AV, Ramage RT, Bohnert HJ, Jensen RG (1991) Purification and characterization of large and small subunits of ribulose 1,5-bisphosphate carboxylase expressed separately in *Escherichia coli*. *Arch Biochem Biophys* **286**: 6–13
23. Streusand VJ, Portis AR (1987) Rubisco activase mediates ATP-dependent activation of ribulose bisphosphate carboxylase. *Plant Physiol* **85**: 152–154
24. Sturdier FW, Rosenberg AH, Dunn JJ, Dubendorff JW (1991) Use of T7 RNA Polymerase to Direct the Expression of Cloned Genes. Novagen (Technical Bulletin), Madison WI